Publishing House
AKAPIT

COMPUTER METHODS IN MATERIALS SCIENCE
Informatyka w Technologii Materiałów

Vol. 18, 2018, No. 2

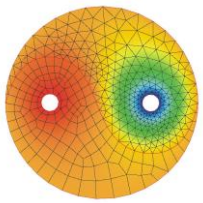

THE IMAGING ALGORITHM FOR THE ULTRASONIC EVALUATION OF METAL CASTINGS BY THE APPLICATION OF AUTOMATED TESTING SYSTEMS BASED ON A SIX DEGREE OF FREEDOM ROBOTIC MANIPULATORS

DMITRY DOLMATOV*, VADIM ZHVYRBLYA, DMITRY SEDNEV, MICHAEL KROENING

National Research Tomsk Polytechnic University, 30, Lenin Ave. Tomsk, Russia
**Corresponding author: dolmatovdo@tpu.ru*

Abstract

Complex-shaped surface represents one of the challenges in ultrasonic testing of metal castings. This conditions the growing interest in development and application of the automated testing system based on a six degrees of freedom (DOF) robotic manipulators. This is due to their ability to provide ultrasonic scanning of the curved specimens with high speed. Higher reliability of the results can be obtained via implementation of the imaging algorithms based on Synthetic Aperture Focusing Technique (SAFT) in the named systems. This approach allows to obtain high-resolution imagery of the internal structure of controlled objects with reduced level of grain noise, the latter occurs due to the often encountered coarse-grained structure of metal castings. In this paper, we introduce the novel imaging algorithm for the automated ultrasonic testing system based on a six degree of freedom robotic manipulator. The capabilities of the algorithm were verified by the application of computer simulations in CIVA 2016 software and also via the in situ experiments. In all the cases analyzed the results revealed that the imaging algorithm allows to make precise imagery of the internal structure of the specimens with different curvature. The obtained research results confirmed the suggested algorithm effectiveness, thus making it acceptable for prospective industrial applications.

Key words: Ultrasonic nondestructive testing, Ultrasonic imaging, Synthetic Aperture Focusing Technique, Automated ultrasonic testing systems, Six degree of freedom robotic manipulators, Complex-shaped objects, Metal castings

1. INTRODUCTION

Ultrasonic nondestructive testing is extensively used in aerospace, petrochemical and power generation industries. One of the areas of ultrasonic evaluation application is metal castings testing. Testing of such objects faces numerous challenges. Firstly, such materials surfaces usually have high roughness. In this case, preliminary mechanical operation of surfaces is necessary to enable the effective ultrasonic nondestructive evaluation. Secondly, such objects are most frequently coarse-grained. For this reason, the extensive grain noise is present in ultrasonic signals making evaluation of testing results more difficult. Thirdly, metal castings commonly have complex-shaped form. In this regard, there is an interest in development and application of the automated systems based on six DOF robotic manipulators. Application of such equipment enables to perform fast automated evaluation of the objects with different shape.

Nowadays the development of ultrasonic testing systems based on six DOF robotic manipulators is predominantly aimed at nondestructive evaluation of composite materials. Existing prototypes and industrial equipment are based on numerous solutions which include various techniques of ultrasonic testing (pulse-echo and through-transmission evaluation), different approaches for acoustic waves generation (air coupled and laser ultrasonic, coupling via

 ISSN 1641-8581

the immersion liquid) and types of ultrasonic transducers (single transducers and phased arrays) (Cuevas et al., 2016; Mineo et al., 2015; Mineo et al., 2016; Mineo et al., 2017). In our earlier work we considered the application of six DOF robotic manipulator for the ultrasonic testing of carbon fiber composites using the pulse-echo ultrasonic testing technique and focused transducer. The obtained precise and accurate imagery of the artificial flaws in the specimen demonstrates the working capacity of the developed testing system prototype (Dolmatov et al., 2016).

However, the approaches developed for ultrasonic testing of the composite materials are not highly effective in the case of metal castings evaluation due to the features of such objects discussed above. For instance, application of focused transducers in testing of composite materials is conditioned by the necessity to obtain high lateral resolution of results and it is effective due to relatively small thickness of such objects. However, metal castings commonly have great thickness. With focused transducers application, significant decrease of lateral resolution will be obtained outside of the focal zone.

In this regard, application of Synthetic Aperture Focusing Technique (SAFT) in automated systems based on 6 DOF robotic manipulators during metal castings testing is of considerable interest. Firstly this approach enables to provide the uniform resolution which does not depend on the depth and is determined only by the physical size of the probe (Schmitz et al., 2000). Secondly, testing results can be presented in the form of imageries which simplifies the evaluation task. Thirdly, application of SAFT allows to reduce the grain noise in comparison with raw ultrasonic data (Stepinski, 2007a).

Practical implementation of SAFT strongly depends on the testing conditions which include the features of applied testing equipment, type of utilized acoustic contact and shape of the controlled object. In general, there are two approaches of SAFT algorithm implementation. Such algorithms can be based on the calculation in the time domain or in the frequency domain (Stepinski, 2007b). The time-domain or delay-and-sum algorithms represent more common approach in ultrasonic imaging and presuppose division of the imaging volume into the voxels and calculation of the delay time related to each voxel (Doctor et al., 1986).

The ultrasonic imaging via the time-domain algorithms in the case of contact ultrasonic testing where the ultrasonic transducer is placed directly on the testing object is straightforward. However, immersion ultrasonic testing or wedges application is more complex as the phenomenon of ultrasonic waves refraction on the interfaces is to be taken into consideration (Kvasnikov et al., 2013; Rougeron et al., 2014)

The frequency-domain algorithms enable higher computation speed in comparison with delay-and-sum imaging algorithms (Langenberg et al., 1986). The first ones are based on the application of the Fast Fourier Transform. In general, imaging in the frequency-domain can be performed by the application of Phase Shift Migration approach or via the Stolt transform. Utilization of Stolt transform is more computationally efficient whereas the imaging via Phase Shift Migration can be efficiently performed in the case of velocity variations in imaging geometry which takes place in immersion ultrasonic testing (Skjelvareid et al., 2011). However, the ultrasonic imaging of the specimens with nonplanar surfaces through Phase Shift Migration cannot be utilized directly. In this regard, Phase Shift Migration approach requires modifications. For this reason, Lukomski (2014) introduced the Non-Stationary Phase Shift Migration Algorithm for the frequency-domain imaging of complex-shaped objects. However, in this algorithm, the iterative procedure is implemented which requires the direct and inverse Fast Fourier Transform on every loop of algorithm operation. This fact strongly impacts the computational speed.

However, algorithms based on SAFT have not been introduced in relation to ultrasonic inspections of automated systems based on six DOF robotic manipulators so far. Nowadays the application of such approach is limited only by medical applications. The capability of SAFT is studied for the 3D model of knee joint determination for the needs of robotic knee arthroplasty. Kerr et al. (2016) and Kerr et al. (2017) demonstrated that application of robotic testing systems and SAFT enables provision of accurate models. Their precision is close to the one of the models obtained via Computer Tomography which is the most common technique in robotic knee arthroplasty nowadays. Nevertheless, in this case, imaging occurs in a homogeneous media and does not comprehensively meet all the requirements of robotic ultrasonic testing.

In this paper, we introduce the imaging algorithm based on SAFT principles for robotic ultrasonic testing systems application to metal castings test-

ing. It incorporates all the features related to such equipment usage.

2. MATERIALS AND METHODS

2.1 Synthetic aperture focusing technique implementation for the robotic ultasonic testing system

The most appropriate approach for the SAFT algorithm implementation for the automated testing system based on 6 DOF robotic manipulators was chosen taking into consideration the features of the testing conditions. The imaging should take place with the respect of the curved surface of the testing specimen and presence of the areas with various acoustical properties in the testing geometry (immersion liquid and testing object). Further, changing of the ultrasonic probe orientation during scanning should be taken into account in the algorithm. In this case application of time-domain approach is more appropriate. It is conditioned by the fact that the complex-shaped surface of the testing object does not allow to use frequency-domain calculation effectively. Another important advantage is the time-domain algorithms transferring to parallel computing units (CUDA, FPGA) which is important for further development of the considered approach (Amaro et al., 2015; Martín-Arguedas et al., 2012).

The general idea of time-domain imaging is the splitting of the imaging area into the voxels and calculation of the time required for ultrasound propagation from the probe to the voxel and back. In the case automated robotic systems it is necessary to perform volumetric ultrasonic imaging. The data available from the electronic unit after scanning includes A-scans, the target point coordinates in the base coordinate system of the robotic manipulator (x_T, y_T, z_T) and the rotation angles of ultrasonic probe around the *Z*-axis (angle α), around the *Y*- axis (angle β) and around the *X*-axis (angle γ). Figure 1 represents the imaging geometry in the single scanning position. The center of the ultrasonic probe is located in point A in such a way that its acoustic axis is perpendicular to the plane around the target point O and crosses this point. B is the point on the interface between the water and the testing object where the refraction takes place and the shortest propagation time between the ultrasonic transducer and the current voxel is reached (according to the Fermat principle).

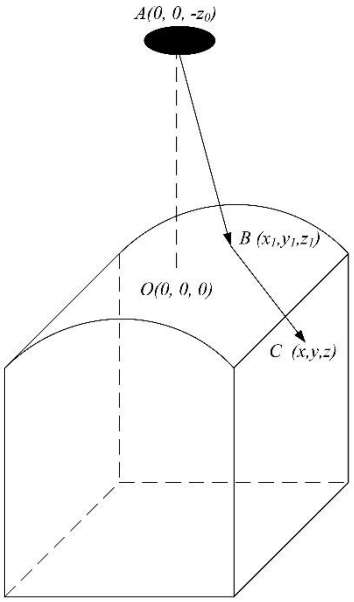

Fig. 1. *The imaging geometry of ultrasonic imaging in the single position of the probe.*

Considering that the target point is the origin of the coordinate system it can be supposed that the position of the probe center (point A) can be described via the coordinates (0;0;-z_0). The determination of two-way travel time between the voxel in imaging volume (point C(*x*,*y*,*z*)) and ultrasonic transducer can be done in the following way:

$$\tau_{xyz} = 2\left(\frac{|AB|}{c_1} + \frac{|BC|}{c_2}\right) \quad (1)$$

where: c_1, c_2 - the velocity of the ultrasonic waves in the water and in the testing specimen (longitudinal waves) respectively.

Due to the fact that the coordinates of the current voxel and the center of the transducer are known it is necessary to determine the coordinates (x_1,y_1,z_1) of the refraction point B which is situated on the surface of the specimen. For this purpose the following function can be introduced:

$$\partial(x', y', z') = \left|\hat{v}_r - \hat{v}'\right| \quad (2)$$

where: $\hat{v}_r$ - the normalized vector, which describes the propagation of the ray refracted on the point *B*'(*x*',*y*',*z*') on the surface of the specimen, $\hat{v}'$ - the normalized vector which connects points *B*'(*x*',*y*',*z*') and *C*(*x*,*y*,*z*) (figure 2).

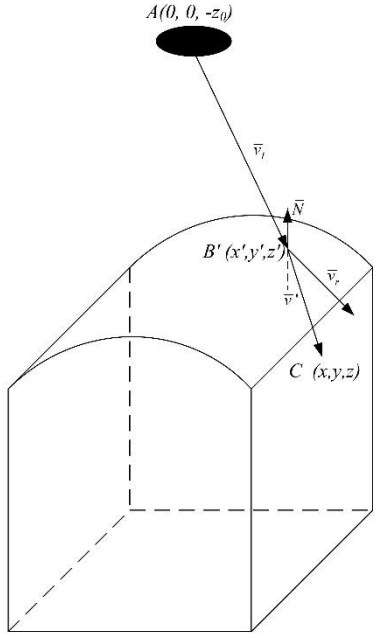

Fig. 2. *Vectors* $\bar{v}_r$ *and* $\bar{v}'$.

The normalized vector $\hat{v}_r$ can be found via the Snell's law in vector form:

$$\hat{v}_r = \frac{c_2}{c_1}[\bar{N} \times (-\bar{N} \times \hat{v}_I)] - \bar{N}\sqrt{1-\left(\frac{c_2}{c_1}\right)^2 (\bar{N} \times \hat{v}_I) \cdot (\bar{N} \times \hat{v}_I)} \tag{3}$$

where: $\hat{v}_I$ - the normalized vector describing the propagation of the incident ray, $\bar{N}$ - the unitary normal vector to the surface in point B'.

In this case, the aim of finding the coordinates of the refraction point B, which corresponds to the specific voxel, is to solve the minimization problem of the function $\delta(x',y',z')$:

$$(x_1, y_1, z_1) = \underset{x',y',z' \in \mathbb{R}}{\arg\min}\left[\delta(x', y'.z')\right] \tag{4}$$

It is possible to solve this task by application of the numerical methods, e.g. the coordinate descent method.

For determining the imagery in the single position, the described approach should be implemented to all voxels in the imaging volume. In order to take the total imagery of the volume of interest, it is necessary to make a summation of partial imagery obtained for various positions of the ultrasonic transducer. For this purpose, the coordinates which describe each voxel should be transformed to the base coordinates system of the robotic manipulator:

$$\begin{pmatrix} x_b \\ y_b \\ z_b \end{pmatrix} = R_{xyz}\begin{pmatrix} x \\ y \\ z \end{pmatrix} + \begin{pmatrix} x_T \\ y_T \\ z_T \end{pmatrix} \tag{5}$$

where: R_{xyz} - the rotation matrix, which can be obtained via multiplication of the rotation matrixes along each of the axis:

$$R_{xyz} = R_z R_y R_x = \begin{pmatrix} \cos\alpha & -\sin\alpha & 0 \\ \sin\alpha & \cos\alpha & 0 \\ 0 & 0 & 1 \end{pmatrix} \times \begin{pmatrix} \cos\beta & 0 & \sin\beta \\ 0 & 1 & 0 \\ -\sin\beta & 0 & \cos\beta \end{pmatrix} \times \begin{pmatrix} 1 & 0 & 0 \\ 0 & \cos\gamma & -\sin\gamma \\ 0 & \sin\gamma & \cos\gamma \end{pmatrix} \tag{6}$$

Determination of partial imagery in the base coordinates of the robot for all positions of the ultrasonic transducer allows obtaining the total imagery of the testing object:

$$I_{total} = \sum_{i=1}^{N} I_i(x_b, y_b, z_b) \tag{7}$$

It is possible to solve this task by application of the numerical methods, e.g. the coordinate descent method.

2.2 The robotic ultrasonic system description

The current automated ultrasonic testing system consists of the six DOF robotic manipulator, the immersion bath, and the control cabinet (figure 3).

Fig. 3. *The current robotic system (1 – robotic manipulator, 2 – immersion bath, 3 – control cabinet).*

The robotic manipulator KUKA KR 10 1100 SIX ensures the movement of the ultrasonic probe during the testing. Six-axis construction of the robot-

ic manipulator allows to perform scanning via the complex trajectory with the respect to the curved surface of testing specimen. The control cabinet includes the electronic unit, robot controller KR4, uninterruptible power supply unit, control desk and the computer. During testing the specimen is placed in the immersion bath filled with water. The average scanning speed is 74 mm per second. However, it heavily depends on the shape of the specimen.

Building-up the necessary scanning trajectory requires the CAD and STL model of the specimen as well as the calibration procedure aimed at determination of the specimen position with respect to the robotic manipulator. The calibration procedure implies determination of the coordinates of specific points of the specimen (corners or artificial tags). For this purpose, the special tool is used which contacts with the points on the testing specimen. Obtained coordinates are juxtaposed with the STL model of the specimen and translation and rotation parameters can be determined.

For creation of the scanning trajectory, the CimStation software is used. For this purpose, the models of the immersion bath, robotic manipulator, and the controlled object are needed to be uploaded to the software workspace. Location of the testing specimen is defined with the respect of the parameters obtained via the calibration procedure. In the CimStation software the conditions related to the ultrasonic echo-signals registration procedure are set including selection of the surface to be scanned and the scanning grid parameters. Furthermore, the trajectory is verified for the possibility of the robotic manipulator to reach every point of the scanning grid and the lack of collisions. The ultrasonic data sampling is carried out via the electronic unit.

3. EXPERIMENTAL SETUP

The suggested algorithm was implemented in Matlab R2017b. The input data for the algorithm is the set of A-scans, coordinates of the target points on the testing specimens and the orientation angles of the ultrasonic probe in each position.

The verification procedure of the suggested algorithm was conducted through the computer simulations as well as via the in situ experiments. The computer simulation application is aimed at testing the impact of the specimen's curvature on the suggested algorithm performance. The input raw ultrasonic data was generated by the application of CIVA 2016 software. It is a powerful and versatile tool which allows varying the types of applied probes and curvature of controlled objects (figure 4) (Mahaut et al., 2009).

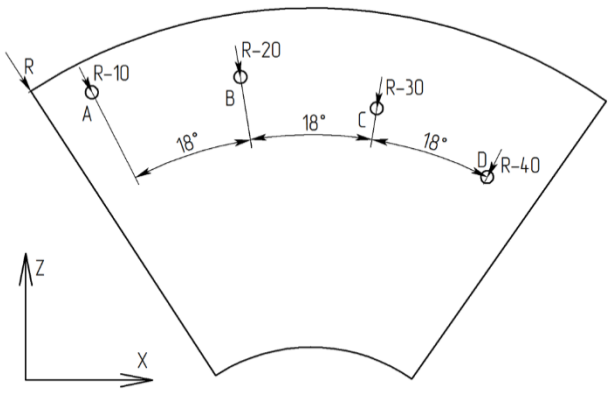

Fig. 4. *The testing specimen with the flaws location in simulations.*

The simulations were performed for testing the specimen's radius variation. In total for testing four curvature radii of 100, 150, 200 and 250 mm were considered for the specimens. In all the cases the side drilled holes are placed as presented in figure 4. As the ultrasonic probe, the 2.25 MHz ultrasonic transducer with 6 mm diameter of piezoelement was used. Scanning took place with the step of 1 mm along the X-axis. In each position, the ultrasonic transducer was oriented perpendicular to the surface of the testing object.

Testing of the algorithm's performance by application of the in situ experimental data was conducted in two stages. The aim of the first stage is to demonstrate the ability of the suggested algorithm to make three-dimensional imaging and check the resolution which can be obtained via the algorithm application. During this stage, the algorithm performance was tested for the steel cast plane block imaging where seven flat bottom holes with the diameter of 4 mm were drilled. The dimensions of the specimen as well as the positions of the flaws are presented in figure 5. The ultrasonic data registration took place according to the grid which provided the distance of 1 mm between the closest sampling points; it covers the whole area of the testing specimen surface.

The second stage is aimed at the evaluation of the suggested algorithm performance for the objects with nonplanar surfaces imaging. For this purpose, the steel cast cylindrical specimen was used. This testing object contains three side-drilled holes with the diameter of 4 mm (figure 6). The scanning grid

covers thirty degrees of the cylinder surface diameter in the radial direction. The distance between two neighboring sampling points was 1 mm along the *X*-axis.

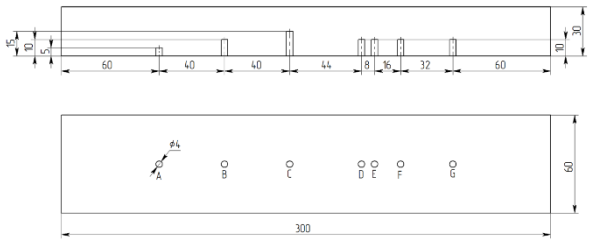

Fig. 5. The dimensions of the plane testing object with the flaws location.

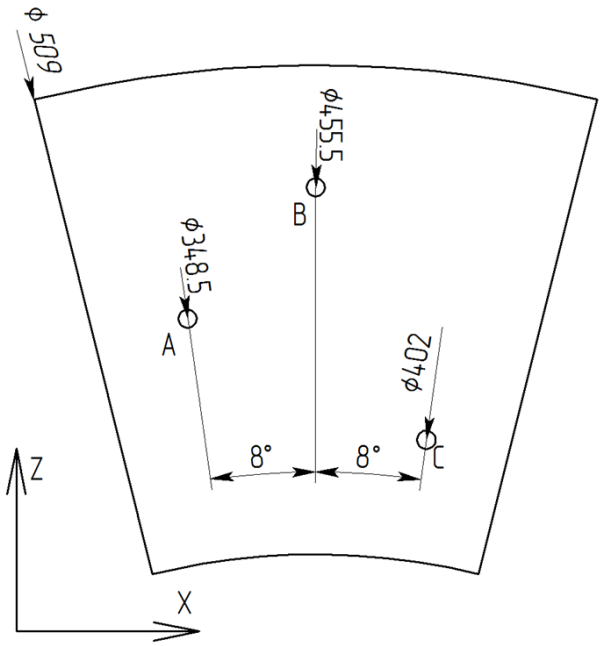

Fig. 6. *The dimensions of the cylindrical testing object with the flaws location.*

During both stages of verification, the ultrasonic transducer with the central frequency of 2.25 MHz and 6 mm in diameter was used for data sampling.

2. RESULTS AND DISCUSSION

Figure 7 presents the results of the algorithm implementation to the simulated ultrasonic data for the various curvature of the testing specimens. All of the results are normalized to the maximum value and amplified by 20 dB.

In order to evaluate the obtained results the Array Performance Indicator criterion can be used (Guarneri et al., 2015). It is calculated for each of the flaws individually and can be expressed via the following relation:

$$API = \frac{S_{-6dB}}{\lambda^2}, \tag{8}$$

where: S_{-6dB} - the area where the amplitude of point-spread function exceeds the -6 dB threshold of the local maximum, cm^2, λ - the wavelength of the sound inside the controlled object, cm.

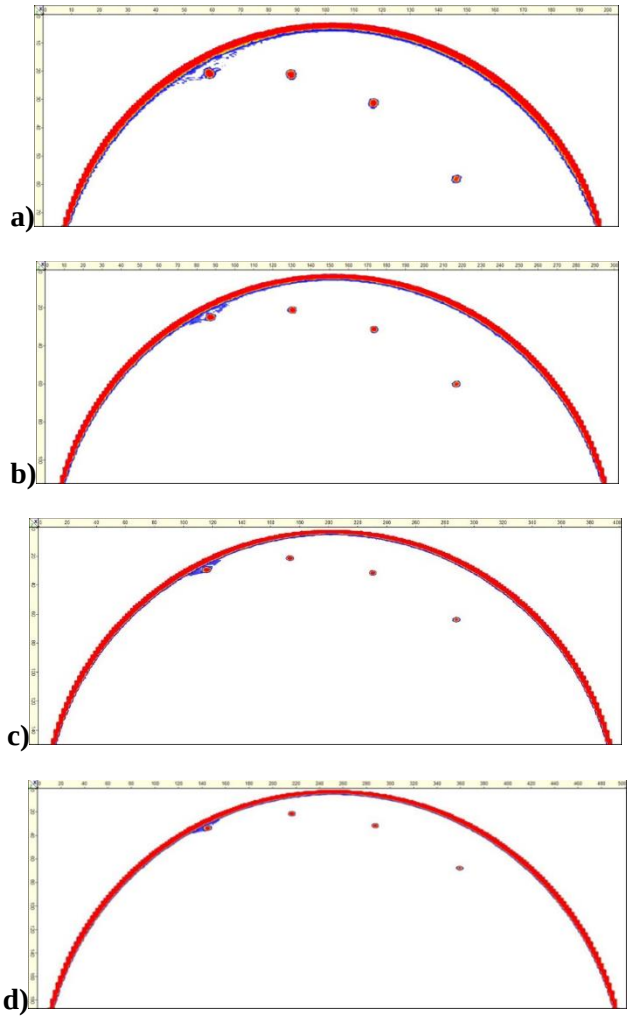

Fig. 7. *The results of algorithm implementation to the raw simulated ultrasonic data: (a) Radius of the specimen is 100 mm; (b) Radius of the specimen is 150 mm; (c) Radius of the specimen is 200 mm; (d) Radius of the specimen is 250 mm.*

The results of API for the flaws are presented in table 1 and figure 8.

Table 1. *API for the flaws in the specimens.*

Flaw	API			
	R=100	R=150	R=200	R=250
A	1.98	1.97	1.99	1.99
B	2.05	2.03	2.07	2.10
C	2.01	2.07	2.09	2.06
D	2.08	2.06	2.04	2.11

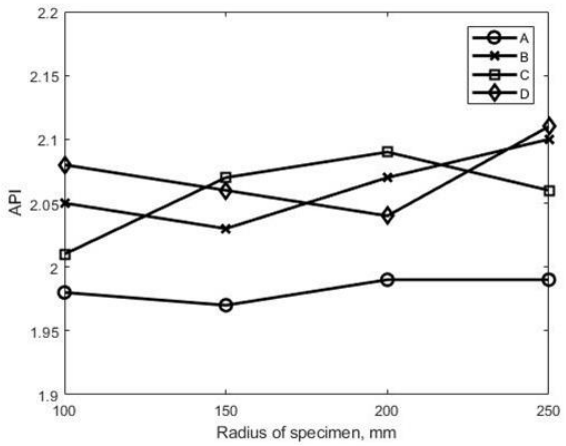

Fig. 8. *API for the flaws in the specimens.*

The results obtained via the computer simulations reveal that precise and accurate imaging of the flaws was obtained for all considered radii of the testing specimen by the application of the suggested algorithm. The algorithm performance analysis through the determination of flaws' API demonstrates that these values lie within the close range from 1.97 to 2.11. This validates the ability of the suggested algorithm to make effective ultrasonic imaging of the testing objects with various curvatures of the surface.

The results obtained via the computer simulations were verified through the in situ experiment. Figure 9 presents the volumetric result obtained for the steel block whereas figure 10 demonstrates the C-scan of this result.

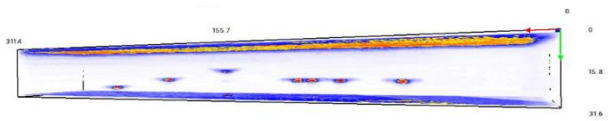

Fig. 9. *The steel block volumetric imagery obtained via the suggested algorithm implementation.*

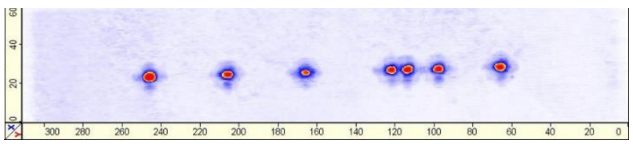

Fig. 10. *The C-scan of the obtained volumetric result of the algorithm implementation.*

Having analysed the data presented in figures 9 and 10 it is possible to conclude that application of the algorithm allowed to separate all the flaws in the imagery. This corresponds to the theoretical lateral resolution of Synthetic Aperture Focusing Technique which is limited by the half of the ultrasonic transducer diameter. In our case, this value is 3 mm.

However, the case of the plane block does not provide the exhaustive evaluation of the suggested algorithm performance. Thus, the secondary study was conducted with the cylindrical specimen. In figure 11 the results of the cylinder specimen imaging are presented.

The obtained results for the cylinrical specimen demonstrate the ability of the suggested algorithm to take into account the specific features of the robotic ultrasonic system which include the presence of the immersion liquid layer and change of the ultrasonic probe orientation during scanning. This conditions the ability of the algorithm to make precise and accurate imaging of complex-shaped objects during testing.

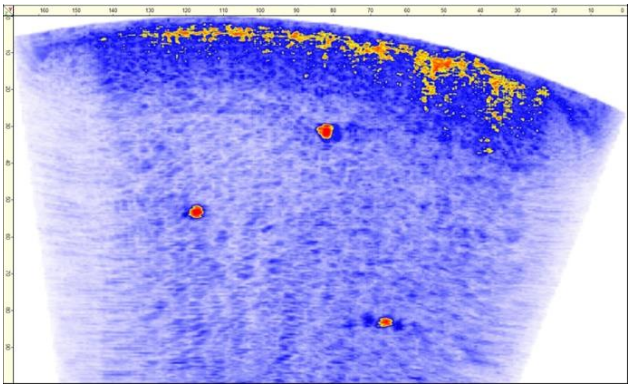

Fig. 11. *The results of the suggested algorithm implementation in the cylinder specimen imaging.*

5. CONCLUSIONS

In this paper, the algorithm of the ultrasonic imaging algorithm for the robotic ultrasonic testing system based on six DOF robotic manipulators is proposed. The suggested algorithm takes into account all the features related to the application of such systems including the curved surfaces of the testing specimens, the presence of the media with different acoustical properties and changes of the transducer orientation during scanning. The suggested algorithm performance was studied in relation to in the framework of metal castings ultrasonic imaging. This study encompassed application of the computer simulations and conducting the in situ experiments. The computer simulation objective was to verify the algorithm effectiveness for the varying curvature of the testing specimen. According to the obtained results and performed ultrasonic imagery analysis, no correlation between the algorithm performance and the curvature of the testing specimen was revealed. The in situ experiments objective was to verify the results obtained via the computer simu-

lations. For this purpose, the ultrasonic imaging of two specimens with different shapes was performed. The accurate and precise imagery of both specimens demonstrates the efficiency of practical implementation of the suggested algorithm.

The obtained results will serve as the basis for further research and development which can be multipurpose. The suggested algorithm acceleration via its transfer onto parallel computer units (CUDA, FPGA) is to be considered. Furthermore, the algorithm adaptation for the phased arrays application is be studied as it enables to improve the quality of testing results and reduce the inspection time when applying this type of ultrasonic transducers.

ACKNOWLEDGEMENTS

The research is funded by the Governmental program "Science", research projects No. 11.3683.2017/4.6 and №11.6342.2017/8.9. The research is carried out within the framework of Tomsk Polytechnic University Competitiveness Enhancement Program.

REFERENCES

Amaro, J., Yiu, B.Y., Falcao, G., Gomes, M.A., Alfred, C.H., 2015, Software-based high-level synthesis design of FPGA beamformers for synthetic aperture imaging, *IEEE T ULTRASON FERR*, 62(5), 862-870.

Cuevas, E., Hernandes, S., Cabellos E., 2016, Robot-based solutions for NDT inspections: integration of laser ultrasonics and air coupled ultrasounds for aeronautical components, *Proc. 25th ASNT Research Symposium*, ed. D. Gilbert, New Orleans, USA, 39-46.

Doctor, S.R., Hall, T.E., Reid, L. D., 1986, SAFT—the evolution of a signal processing technology for ultrasonic testing, *NDT&E INT*, 19(3), 163-167.

Dolmatov, D., Zhvyrblya, V., Filippov, G., Salchak, Y., Sedanova, E., 2016, Advanced ultrasonic testing of complex shaped composite structures, *IOP Conf. Ser. Mater. Sci. Eng*, 135(1), 012010.

Guarneri, G.A., Pipa, D.R., Junior, F.N., de Arruda, L.V.R. Zibetti, M.V.W., 2015, A sparse reconstruction algorithm for ultrasonic images in nondestructive testing. *Sensors*, 15(4), 9324-9343.

Kerr, W., Pierce, S. G., Rowe, P., 2016, Investigation of synthetic aperture methods in ultrasound surface imaging using elementary surface types, *Ultrasonics*, 72, 165-176.

Kerr, W., Rowe, P., Pierce, S.G., 2017, Accurate 3D reconstruction of bony surfaces using ultrasonic synthetic aperture techniques for robotic knee arthroplasty, *Comput. Med. Imag. Grap.*, 58, 23-32.

Kvasnikov, K.G., Soldatov, A.I., Bolotina, I.O., Krening, K.M., Potapenko, A.A., 2013, The use of geometrical acoustics for the solution of visualization problems, *Russ. J. Nondestruct.*, 49(11), 625-630.

Langenberg, K.J., Berger, M., Kreutter, T., Mayer, K., Schmitz, V., 1986, Synthetic aperture focusing technique signal processing, *NDT Int*., 19(3), 177-189.

Lukomski, T., 2014, Non-stationary phase shift migration for flaw detection in objects with lateral velocity variations, *Insight*, 56(9), 477-482.

Mahaut, S., Darmon, M., Chatillon, S., Jenson, F., Calmon, P., 2009, Recent advances and current trends of ultrasonic modelling in CIVA, *Insight*, 51(2), 78-81.

Martín-Arguedas, C.J., Romero-Laorden, D., Martinez-Graullera, O., Perez-Lopez, M., Gomez-Ullate., 2012, An ultrasonic imaging system based on a new SAFT approach and a GPU beamformer, *IEEE T. Ultrason. Ferr.*, 59(7), 1402-1412.

Mineo, C., MacLeod, C., Morozov, M., Pierce, S.G., Lardner, T., Summan, R, Paton, S., 2016, Fast ultrasonic phased array inspection of complex geometries delivered through robotic manipulators and high speed data acquisition instrumentation, *Proc. 2016 IEEE Int. Ultrasonics Symposium*, ed. Freear, S. , Tours, 37-41.

Mineo, C., Pierce, S.G., Wright, B., Cooper, I., Nicholson, P.I., 2015, PAUT inspection of complex-shaped composite materials through six DOFs robotic manipulators, *Insight*, 57(3), 161-166.

Mineo, C., Summan, R., Riise, J., MacLeod, C.N., Pierce, S.G, 2017, Introducing a new method for efficient visualization of complex shape 3D ultrasonic phased-array C-scans, *Proc. 2017 IEEE Int. Ultrasonics Symposium*, ed. Schmitz, G., Washington, 1-4.

Rougeron, G., Lambert, J., Iakovleva, E., Lacassagne, L., Dominguez, N., 2014, Implementation of a GPU accelerated total focusing reconstruction method within CIVA software, *AIP Conf. Proc*., 1581(1), 1983-1990.

Schmitz, V., Chakhlov, S., Müller, W., 2000, Experiences with synthetic aperture focusing technique in the field, *Ultrasonics*, 38(1-8), 731–738.

Skjelvareid, M.H., Olofsson, T., Birkelund, Y., Larsen, Y., 2011, Synthetic aperture focusing of ultrasonic data from multilayered media using an omega-k algorithm, *IEEE T. Ultrason. Ferr.*, 58(5), 1037-1048.

Stepinski, T., 2007a, SAFT performance in ultrasonic inspection of coarse grained metals. *Proc. 6th Int. Conf. on NDE in Relation to Structural Integrity for Nuclear Pressurised Components*, eds., Bieth, M., Whittle, J., Budapest, 8-10.

Stepinski, T., 2007b, An implementation of synthetic aperture focusing technique in frequency domain, *IEEE T. Ultrason. Ferr.*, 54(7), 1399-1408.

ALGORYTM OBRAZUJĄCY DLA ULTRADŹWIĘKOWYCH BADAŃ METALOWYCH ODLEWÓW WYKORZYSTUJĄCY AUTOMATYCZNY SYSTEM TESTUJĄCY Z MANIPULATORAMI O SZEŚCIU STOPNIACH SWOBODY

Streszczenie

Powierzchnie o skomplikowanym kształcie są jednym z wyzwań przy ultradźwiękowym badaniu metalowych odlewów. To wyzwanie spowodowało wzrost zainteresowania automatycznymi systemami badawczymi wykorzystującymi roboty manipulatory o sześciu stopniach swobody. To zainteresowanie wynika z

możliwości tych robotów w zakresie ultradźwiękowego skanowania z dużą prędkością zakrzywionych powierzchni. Wysoka wiarygodność wyników może zostać osiągnięta przez zastosowanie algorytmów obrazujących wykorzystujących syntetyczną technikę skupiania przysłony (ang. Synthetic Aperture Focusing Technique SAFT). Takie podejście pozwaliło na otrzymanie wysokiej rozdzielczości obrazu wewnętrznej struktury badanego obiektu przy obniżonym poziomie szumów, które pojawiają się w przypadku częso spotykanych gruboziarnistych struktur odlewów. W niniejszym artykule opisano nowy algorytm dla automatycznego systemu badań ultradźwiękowych wykorzystującego roboty manipulatory o sześciu stopniach swobody. Możliwości algorytmu zostały zweryfikowane przez wykonane numeryczne symulacje w oprogramowaniu CIVA 2016 oraz przez doświadczenia in situ. Wyniki dla wszystkich analizowanych przypadków potwierdziły, że analizowany algorytm obrazujący pozwala uzyskać precyzyjny obraz wewnętrznej struktury próbek o różnych krzywiznach powierzchni. Uzyskane wyniki potwierdziły efektywność algorytmu i możliwość jego zastosowania w warunkach przemyysłowych.

Received: November 22, 2018.
Received in a revised form: December 19, 2018.
Accepted: December 26, 2018.